Inorganic Chemistry

Article

pubs.acs.org/IC

Photophysical Properties of $\{[Au(CN)_2]^-\}_2$ Dimers Trapped in a Supramolecular Electron-Acceptor Organic Framework

Ahmed S. Abouelwafa,[†,‡,§] Christopher E. Anson,[†] Andreas Hauser,[§] Howard H. Patterson,[⊥] François Baril-Robert,[⊥] Xiaobo Li,[⊥] and Annie K. Powell[†,*,‡]

[†]Institut für Anorganische Chemie, Karlsruhe Institute of Technology, Engesserstrasse 15, D-76128 Karlsruhe, Germany

[‡]Institut für Nanotechnologie, Karlsruhe Institute of Technology, Postfach 3840, D-76021 Karlsruhe, Germany

[§]Département de Chimie Physique, Université de Genève, 30 Quai Ernest Ansermet, CH-1211 Genève, Switzerland

[⊥]Department of Chemistry, University of Maine, Orono, Maine, 04469, United States

Supporting Information

ABSTRACT: Dicyanoaurate reacts with the organic acceptor molecule, 1,1′-*bis*-(2,4-dinitrophenyl)-4,4′-bipyridinium, **DNP**, to form a supramolecular complex with the general formula $\{[Au(CN)_2]_2\mathbf{DNP}\}\cdot 4H_2O$. The complex was characterized by X-ray crystallography, and its photophysical properties were investigated in the solid-state. Although the initial $(\mathbf{DNP})Cl_2$ compound does not show photoluminescence behavior and the dicyanoaurate shows photoluminescence only in the UV range, the resulting supramolecular complex displays two simultaneous, essentially independent, photoluminescence bands in the visible range originating from individual contributions of the **DNP** unit and the dicyanoaurate dimers. This unusual simultaneous photoluminescence behavior displayed by both the dicyanoaurate donor units and the redox-active 4,4′-bipyridinium acceptor have lifetimes of 0.5 μs and several hundred μs, respectively.

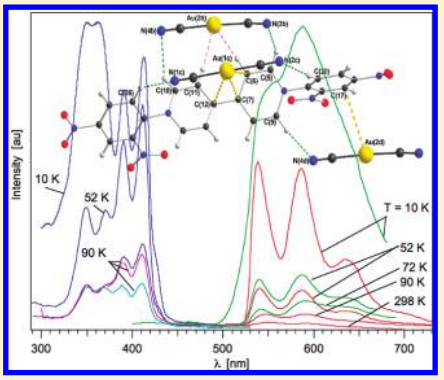

INTRODUCTION

Dicyanoaurate(I) is one of the most stable two-coordinate complexes of transition metal ions. It has attracted a great deal of attention because of its potential in both scientific and industrial applications such as crystal engineering,[1] semiconductors, and functional materials.[2] The diverse applications of this complex result from both its electronic[3] and its geometric structure allowing for two possible binding sites, thus offering a further means to control both the supramolecular structure and the electronic properties in a variety of organic−inorganic[4] and metal-CN-metal[5] charge-transfer materials. The geometry of dicyanoaurate as a linear, small building block with two potential cyano-coordination sites has enabled its use as a bridging unit to form a series of coordination polymers with interesting magnetic properties.[6] Meanwhile, the d^{10} Au(I) metal center in the dicyanoaurate ion is known to favor the formation of $[Au(CN)_2^-]_n$ aggregates through aurophilic interactions thus offering a possibility to control the dimensionality[1,7] and to tune the optical properties in a series of charge-transfer, luminescent aggregates in solution and in the solid state.[8]

These properties were reported for a variety of organic−inorganic hybrid materials containing innocent, redox-inactive organic ligands. In the search toward functional materials with novel electronic and optical properties, we decided to investigate the system consisting of dicyanoaurate with non-innocent, redox active organic electron acceptors such as viologens. Viologens are strong electron acceptors that can form ion-pair charge transfer complexes (IPCT) with electron donors[9−11] having a wide range of applications in charge-separation[10] and in the development of photo-[9] and electrochromic devices.[11]

The majority of studies focusing on the *optical properties* of viologens were performed in solution.[9,10b−h] This includes the photoinduced reduction of viologens in IPCT complexes,[9] the different factors influencing the mechanisms and dynamics of this photoreduction, and hence their optical properties. Ferraudi et al. studied the factors influencing the formation of the methylviologen radical cation and its decay kinetics in aqueous and methanolic solutions.[10h] The spectroscopic and flash photolysis studies performed by Ferraudi and others[10b−g] showed that the photochemical reduction of the viologen takes place by intermolecular electron transfer from the counteranion to the viologen core leading to the formation of the viologen radical cation.

A particularly interesting behavior, though less explored, is the fluorescence of viologens. The detailed dynamics and factors influencing the fluorescence behavior of viologens have been reported in different solvent media[12a] and for viologens incorporated into either zeolites[12b,c] or the interlamellar spaces of hectorite and montmorillonite clays suspended in water.[12d]

Meanwhile, many solid state studies of viologen CT complexes involved the use of viologens, mainly alkyl viologen, as acceptor with organic[9d,e] or inorganic[9a−c,13a] donors to form IPCT complexes displaying common, nonquantified charge transfer phenomena.[9,13]

Received: May 25, 2011
Published: January 19, 2012

   dx.doi.org/10.1021/ic201109u | *Inorg. Chem.* 2012, 51, 1294−1301

Phenyl-viologens with extended π-conjugated fragments have shown more promising optical and electronic properties than the corresponding alkyl derivatives.[10a,14] Some of these phenyl-viologens were also found to fluoresce in solution.[14e,f] The photophysical properties of these viologen compounds, and the luminescence behavior in particular, remain less explored even in solution.[9a,12] This is because photoexcited viologens are formidable oxidants with an estimated reduction potential of 3.65 V vs NHE for the methyl derivative in comparison to −0.45 V vs NHE for the ground-state (i.e., nonphotoexcited state) of the same derivative.[12a] In fact, the strong electron accepting properties of viologens make them very strong fluorescence quenchers for triplet exciplexes of porphyrin,[15a,b] the triplet metal−ligand charge transfer (^{3}MLCT) luminescence of tris(bipyridyl)-ruthenium(II) complexes,[15c−e] and for conjugated rotaxanes.[15f] Similarly, Petersson et al. have recently reported photoinduced electron transfer reactions in a self-assembled Zn(II) porphyrin-viologen complex in aqueous solution.[15g,h] Even more recently some reports discussed the quenching of the luminescence of several gold(I) mono-, and trinuclear complexes by different viologen derivatives.[15i]

To extend our recently published solid-state studies on the supramolecular complexes formed between the viologen derivative 1,1′-*bis*-(2,4-dinitrophenyl)-4,4′-bipyridinium dichloride, (**DNP**)Cl_2, and hexacyanoferrate,[10a] we decided to combine the viologen derivative with the optically interesting dicyanoaurate(I) anion. The **DNP** viologen derivative is particularly interesting because of its extended π-conjugated phenyl fragments, which together with the four peripheral nitro groups allow for both an increase of the electron accepting potential of the 4,4′-bipyridinium core and a further decrease of the energy of the lowest unoccupied molecular orbital (LUMO) of the overall π-conjugated molecule, thus enhancing its interaction with the gold metal orbitals. We report here the luminescence properties in a supramolecular assembly of the dinitrophenyl-viologen **DNP** and dicyanoaurate(I) in the solid state, in which the viologen acceptor phosphorescence is displayed by the viologen acceptor in addition to dicyanoaurate(I) dimer emission.

EXPERIMENTAL SECTION

Synthesis. The reaction of stoichiometric equivalents of the viologen 1,1′-*bis*-(2,4-dinitrophenyl)-4,4′-bipyridinium dichloride, (**DNP**)Cl_2[10a] (0.021 g, 0.033 mmol) dissolved in 30 mL of distilled water with potassium dicyanoaurate (0.019 g, 0.066 mmol) immediately results in the formation of the compound {$[Au(CN)_2]_2$-**DNP**}·$4H_2O$ (**1**) in microcrystalline form in 60% yield. Crystals suitable for X-ray crystallographic analysis were collected from the mother liquor after filtration and leaving the solution for one week. *Elemental analysis.* calcd for $C_{26}H_{14}Au_2N_{10}O_8·2H_2O$: C, 30.48; H, 1.77; N, 13.67, found: C, 30.38; H, 1.65; N, 13.51. The amounts of carbon, nitrogen, and hydrogen in all samples were quantitatively analyzed using an *Elementar Vario EL* analyzer.

X-ray Crystallography. The supramolecular complex **1** immediately forms as microcrystals on mixing the components with single crystals obtained after leaving the supernatant for one week. Comparison of the powder diffraction pattern from the microcrystals with the simulated pattern calculated from the single-crystal structure (see Supporting Information, Figure S1) showed that both have the same crystal structure and that the precipitated material is phase pure.

The crystals obtained after filtration of the solution are nonetheless still rather small and weakly diffracting, and invariably pose problems due to twinning. Most crystals were found to form multiple twin domains by rotations about more than one axis resulting in the diffraction streaking between reflections from different domains. After many attempts (including using a synchrotron source) a crystal was identified as nearly single and could be measured using very long exposures on a rotating anode source to give a structure which could be refined to acceptable R-factors. The residual twinning is the reason why there is some significant electron density near the Au atoms in the final difference map as well as larger than ideal esds on the bond lengths and angles.

Data were measured at 150(2) K on a Stoe IPDS II diffractometer using graphite-monochromated Mo-*Kα* radiation from a rotating anode source. Structure solution by direct methods and full-matrix least-squares refinement were carried out using the SHELXTL package.[16] All non-H atoms were refined with anisotropic thermal parameters. Organic H-atoms were placed in calculated positions; no attempt was made to locate the H-atoms on the lattice water molecules. Details of the data collection and structural refinement are summarized in Table 1. Crystallographic

Table 1. Crystal Data for 1

formula	$C_{26}H_{22}Au_2N_{10}O_{12}$
formula weight	1060.47
crystal system	monoclinic
space group	$P2_1/c$
a/Å	11.1208(7)
b/Å	26.2449(12)
c/Å	10.9484(7)
β/deg	97.156(5)
U/Å^3	3170.6(3)
Z	4
T/K	150(2)
$F(000)$	2008
D_c/Mg m^{-3}	2.222
μ(Mo−Kα)/mm^{-1}	9.323
data measured	24178
unique data	6716
R_{int}	0.0588
data with $I \geq 2\sigma(I)$	5986
wR_2 (all data)	0.2030
S (all data)	1.065
R_1 [$I \geq 2\sigma(I)$]	0.0678
parameters/restraints	451
biggest diff. peak/hole/e Å^{-3}	+4.24/−3.94

data (excluding structure factors) for the structure in this paper have been deposited with the Cambridge Crystallographic Data Centre as supplementary publication nos. CCDC 787004. Copies of the data can be obtained, free of charge, on application to CCDC, 12 Union Road, Cambridge CB2 1EZ, UK: http://www.ccdc.cam.ac.uk/cgi-bin/catreq.cgi, e-mail: data_request@ccdc.cam.ac.uk, or fax: +44 1223 336033.

Luminescence Spectroscopy. Preliminary solid-state emission and excitation spectra were collected using a Photon Technology International Model QuantaMaster-1046 spectrophotometer and a Janis ST-100 optical cryostat to record emission and excitation spectra at lower temperatures. The temperature dependent emission and excitation spectra shown in this paper were recorded with a Fluorolog 3 (Horiba) luminescence spectrometer with the sample inside a closed cycle cryostat (Oxford Instruments CCC1204). Luminescence decay curves and time-gated luminescence spectra were measured on a home-built system consisting of a 0.27 m single monochromator (Spex M270) for light-dispersion, a PM (Hamamatsu R928) and a multi channel scaler (Stanford Research SR 430) and a photon counting system (Stanford Research SR 400) for detection. For excitation either the third harmonic of a pulsed Nd:YAG laser (Quantel Brilliant B) at 355 nm or the output of a MOPO (Opotek Magic Prism) at 420 nm pumped by the same Nd:YAG laser were used. The overall time resolution of the system was 10 ns.

RESULTS AND DISCUSSION

Crystal Structure. The supramolecular compound forms as a result of the electrostatic interactions between the electron-rich

dx.doi.org/10.1021/ic201109u | Inorg. Chem. 2012, 51, 1294−1301

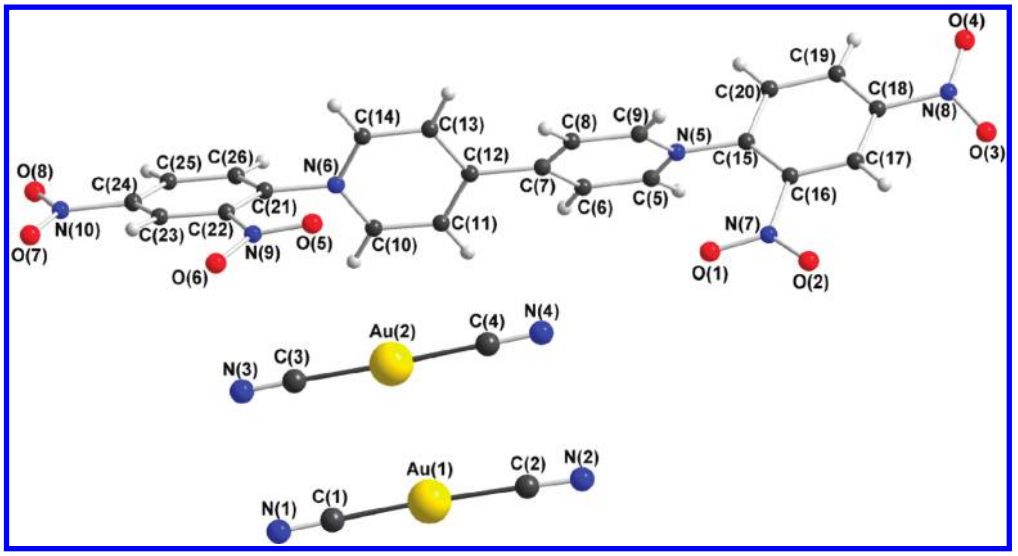

Figure 1. Structure of the DNP^{2+} cation and dicyanoaurate anions in compound **1**, with the atomic numbering scheme.

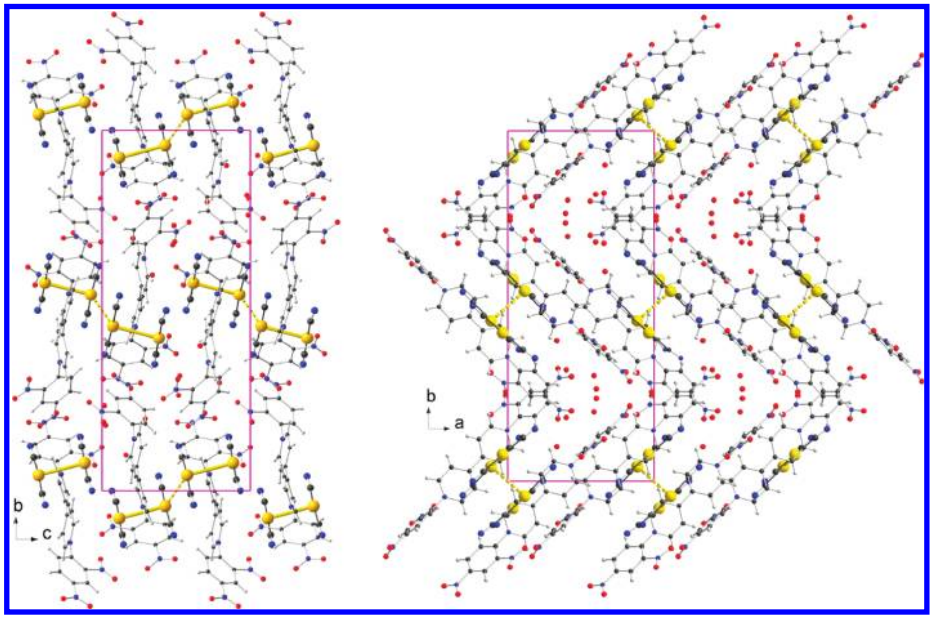

Figure 2. Packing of the supramolecular complex **1** viewed along the *a*-axis (left) and the *c*-axis (right). The 3.5108 Å Au···Au interactions are shown as solid yellow lines; the longer 3.8738 Å interactions are shown dotted. (Au, yellow; C, black; N, blue; O, red; H, white; cyanide C and N atoms are shown larger than organic C and N). Water molecules are omitted for clarity.

dicyanoaurate units and the electron deficient viologen unit. The X-ray crystallographic analysis shows that the asymmetric unit contains two dicyanoaurate units, one **DNP** viologen cation and four water molecules (Figure 1), and the compound is thus formulated as $\{[Au(CN)_2]_2\mathbf{DNP}\}\cdot 4H_2O$. Bond lengths and angles are consistent with the original oxidation states of the two components, namely, $\mathbf{DNP}^{2+}$ and $[Au(CN)_2]^-$.

The $\mathbf{DNP}^{2+}$ cations in **1** are linked via a range of hydrogen bonds involving both pyridinium and phenyl C−H bonds and oxygen atoms from the nitro groups (C···O 3.207−3.329 Å) into corrugated sheets running parallel to the (100) plane (Figure 2). These two-dimensional (2-D) networks act as hosts for the dicyanoaurate anions. The two dicyanoaurate units are crystallographically inequivalent. Both have typical linear geometries, with Au−C bond lengths in the range 2.003(13)−2.028(15) Å and C−Au−C angles of 177.1(5) and 176.2(5)° respectively. The two anions are close to parallel, with the C(1)···C(2) and C(3)···C(4) vectors subtending an angle of only 5.4°. The Au(1)···Au(2) distance is rather short, 3.5108(7) Å, indicating aurophilic interaction between these Au centers (Figure 3a). The sum of the van der Waals radii of two Au(I) centers is 3.60 Å and is thus considered to be the upper limit of a distance for a significant aurophilic interaction.[17a] Patrick et al. studied the gold−gold interactions in a series of heterobimetallic coordination polymers containing Cu^{II} and $[Au(CN)_2]^-$ units.[1] The gold−gold distances in the range 3.14 to 3.59 Å were attributed to aurophilic interactions between the gold centers while molecules with Au···Au distances larger than 3.60 Å were not considered to involve significant aurophilic interactions. Therefore, the complex **1** in the solid state can be thought of as a supramolecular structure containing dimers of dicyanoaurate anions trapped within a viologen framework.

The separation between Au(1) and its symmetry equivalent Au(1a) at $\{-x, -y+1, -z+2\}$ is longer, at 3.8738(9) Å.

dx.doi.org/10.1021/ic201109u | *Inorg. Chem.* 2012, 51, 1294−1301

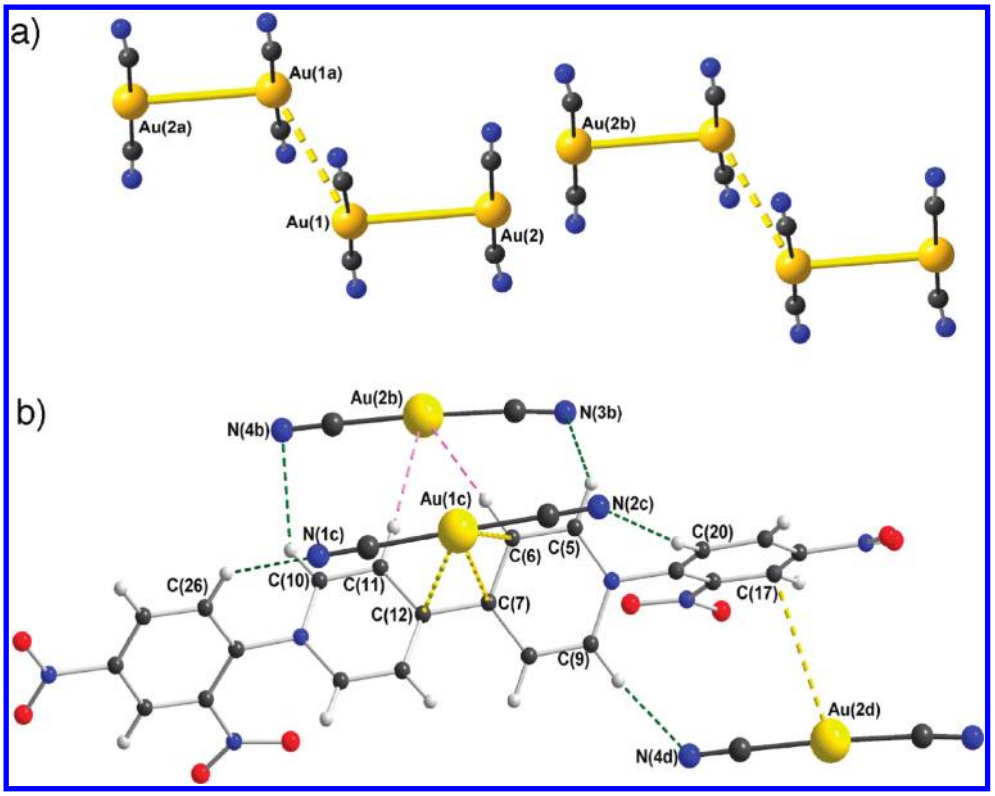

Figure 3. (a) Interactions between the dicyanoaurate complexes in **1**: Au(1)···Au(2) 3.5108(7) Å, Au(1)···Au(1a) 3.8738(9) Å, Au(2)···Au(2b) 4.7681(9) Å, Au(1a)···Au(1)···Au(2) 116.69(2)° (above). (b) Interactions between the $\mathbf{DNP}^{2+}$ viologen cation and neighboring dicyanoaurate complexes; CH···N hydrogen bonds shown in green, C···Au contacts in the range 3.60−3.75 Å in yellow, H···Au contacts under 3.25 Å in pink (below). Symmetry codes: a {−*x*, −*y*+1, −*z*+2}; b {−*x*, −*y*+1, −*z*+1}; c {*x*, *y*, *z*−1}; d {−*x*+1, −*y*+1, −*z*+1}.

However, the distance from Au(2) to its symmetry equivalent at {−*x*, −*y*+1, −*z*+1} is over 4.7 Å, precluding any interaction between these gold centers. With a Au(1a)···Au(1)···Au(2) angle of 116.69(2)°, the dicyanoaurate dimers form a weakly interacting "dimer-of-dimers", with a planar centrosymmetric structure somewhat reminiscent of the butadiene molecule.

The dimers of dicyanoaurate anions are embedded in the network of $\mathbf{DNP}^{2+}$ cations, with each cation interacting significantly with three neighboring dicyanoaurate anions (Figure 3b). The primary interactions involve hydrogen bonding from C−H bonds on the cations to cyanide nitrogen atoms. Particularly noteworthy is the way in which the dicyanoaurate based on Au(1c) (the symmetry-equivalent of Au(1) at *x*, y, *z*−1) is held in place by two hydrogen bonds from phenyl C−H groups, one to each nitrogen, such that the gold center is held over the open face of the dipyridinium moiety, making Au···C contacts to C(6), C(7), and C(12) of 3.630(10), 3.715(10), and 3.706(10) Å, respectively. These are shown as yellow dotted lines in Figure 3b. The dicyanoaurate anion containing Au(2b), on the other hand, accepts hydrogen bonds from two pyridinium C−H bonds and is held alongside the viologen cation, in the plane of the dipyridinium system, such that the C−H bond on C(11) points almost directly at the gold center, with C(11)···Au(2b) 3.829(10) Å, H(11A)···Au(2b) 2.89 Å, and a C−H···Au angle of 169°. The third such interaction involves the dicyanoaurate based on Au(2d), which is also held by a C−H···N hydrogen bond, such that the C(17)···Au(2d) distance is 3.608(10) Å, with Au(2d) lying almost over the phenyl ring. These Au···Au and supramolecular Au···C interactions will be shown to have a substantial effect on the photophysical properties of **1**.

Photophysical Properties. At room temperature compound **1** in crystalline form shows only a very weak broad luminescence at 550 nm upon excitation at 410 nm. At 10 K the luminescence is quite strong and very different emission spectra depending on the excitation wavelength are observed (Figure 4). Upon excitation at 320 nm, that is, in the region typical for strong absorption bands of $[Au(CN)_2]^-$ clusters,[8,17] a strong emission with a first maximum at 370 nm followed by a slightly weaker and very broad, weakly structured emission with a maximum at 588 nm is observed (violet line). For excitation at 360 nm, the broad emission at lower energy continues to be observed (blue line), and finally for excitation at 420 nm (red line), the compound displays structured emission, showing a vibronic progression with emission maxima at 538 nm (18588 cm^{-1}), 586 nm (17065 cm^{-1}), and 634 nm (15773 cm^{-1}). This progression corresponds to aromatic ring C═C stretching normal modes with a frequency in the range of 1300 to 1500 cm^{-1} which are also observed in the IR spectrum of the compound (see the Supporting Information, Figure S2), thus indicating that this emission comes from the $\mathbf{DNP}^{2+}$ viologen organic moiety. This excitation wavelength dependence gives a first indication of the presence of two emitting species in the sample.

To confirm this assumption and to identify each species, excitation spectra of the compound were recorded at three different emission wavelengths at 10 K (Figure 4). For the first one, the emission wavelength λ_{em} was chosen at 390 nm. It shows absorption with effects of saturation below 340 nm and a Stokes shift of around 3500 cm^{-1} (pink line). By comparison with the single crystal absorption spectrum included in Figure 4 (dark green, dotted line), which shows the rise to an intense absorption in the same region, this excitation corresponds to a dipole-allowed transition. As the S_1 transition on $\mathbf{DNP}^{2+}$ is

dx.doi.org/10.1021/ic201109u | *Inorg. Chem.* 2012, 51, 1294−1301

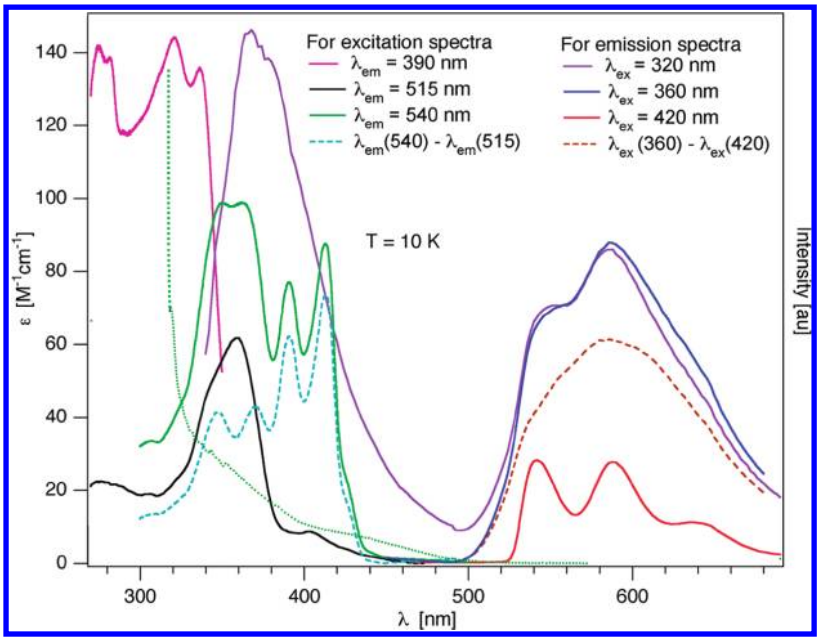

Figure 4. Luminescence and excitation spectra of $\{[Au(CN)_2]_2$**DNP**$\}\cdot 4H_2O$ at 10 K. For luminescence spectra λ_{ex} = 320 nm (violet), 360 nm (blue), and 420 nm (red), for excitation spectra λ_{em} = 390 nm (pink), 540 nm (green), and 515 nm (black). The dotted lines are calculated difference spectra resulting from the subtraction of two spectra measured at the same temperature and different wavelengths as indicated in emission (brown) and excitation (light blue), respectively. The single crystal absorption spectrum at 10 K is shown as green dotted line.

expected at higher energies (Supporting Information, Figure S3) this transition can be tentatively assigned to the lowest excited transition of singlet origin on $[Au(CN)_2]^-$.[17b] For the other two, λ_{em} was chosen at 515 nm because the wing of the broad emission appears exclusively in this range, and at 540 nm (green line) which corresponds to the emission maximum of the structured emission. Indeed, for the latter two very different excitation profiles were observed. The first excitation spectrum recorded at λ_{em} = 515 nm (black line) shows a broad, structureless band in the range 335−370 nm with maximum intensity at 360 nm, and a weaker shoulder to lower energies. The second spectrum measured at λ_{em} = 540 nm (green line) shows four peaks at 412 nm (24271 cm^{-1}), 390 nm (25641 cm^{-1}), 370 (27027 cm^{-1}), and 348 nm (28735 cm^{-1}). In addition there is a large energy gap between the emission and the onset of the absorption.

In what follows, we are mainly interested in the dual nature of the emission in the visible region, that is, between 500 and 700 nm. The time-resolved spectra and luminescence decay curves at different wavelengths shown in Figures 5 and 6 together with the above information clearly indicate that there are two almost independent emissions hidden under the band in the visible: one unstructured and broad centered at 580 nm upon excitation at 355 nm showing nearly exponential decay and a lifetime of 34 μs at 10 K, the other one corresponding exclusively to the structured luminescence observed with irradiation at 420 nm. The latter shows some deviations from single exponential behavior and a tail reaching into the hundreds of microseconds region, and with lifetimes of 44 and 940 μs, respectively, the two emissions must correspond to forbidden transitions, that is, phosphorescence. A fast initial decay with a lifetime of 0.34 microseconds for excitation at 355 nm and detection at 510 nm (Figure 6, inset) is also observed. This is due to the tail of the UV luminescence. Its lifetime is in line with the postulated fluorescence of the gold cluster.[17c]

The information allows us to conclude that the excitation spectrum with λ_{em} = 515 nm corresponds to a pure excitation spectrum of the species with a lifetime of ~34 μs, whereas the excitation spectrum with λ_{em} = 540 nm is a superposition of the spectra of the two species. Conversely, the structured luminescence spectrum with irradiation at λ_{ex} = 420 nm corresponds exclusively to the species with the long lifetime, whereas the luminescence spectrum with λ_{ex} = 355 nm is a superposition of the luminescence of the two species. The luminescence spectrum of the fast decaying species and the excitation spectrum of the slowly decaying species can now be estimated as weighted difference spectra. These are shown as dashed lines in Figure 4.

The facts that (a) at 10 K both emissions in the range from 500 to 700 nm are comparatively strong, (b) the relative intensities of the bands in emission and excitation at 10 K are reproducible for different preparations of the sample ranging from a quickly precipitated fine powder sample to slowly crystallized microcrystalline material, and (c) the spectra do not change with the duration or irradiation, indicate that both types of luminescence are due to intrinsic properties of the material and not to impurities or photochemical products. We have previously reported[3b] that defect site emission can occur with powders but not with crystalline material, so we conclude the emission is due to the material.

Temperature dependent emission and excitation spectra (Figure 7) confirm the dual nature of the luminescence in the visible region. In addition to an overall decrease in luminescence intensity with increasing temperature, the unstructured luminescence at 580 nm is quickly quenched as the temperature is raised above 50 K, and the excitation spectrum of the remaining structured luminescence is identical to the difference spectrum shown in Figure 4 (also Supporting Information, Figure S4). The unstructured band in emission and its counterpart in excitation can be attributed to an excitonic state of formally triplet origin of the dicyanoaurate dimers, consistent with reported excitation spectra for dicyanoaurate aggregates[8a,17d,e] and coordination polymers

dx.doi.org/10.1021/ic201109u | Inorg. Chem. 2012, 51, 1294−1301

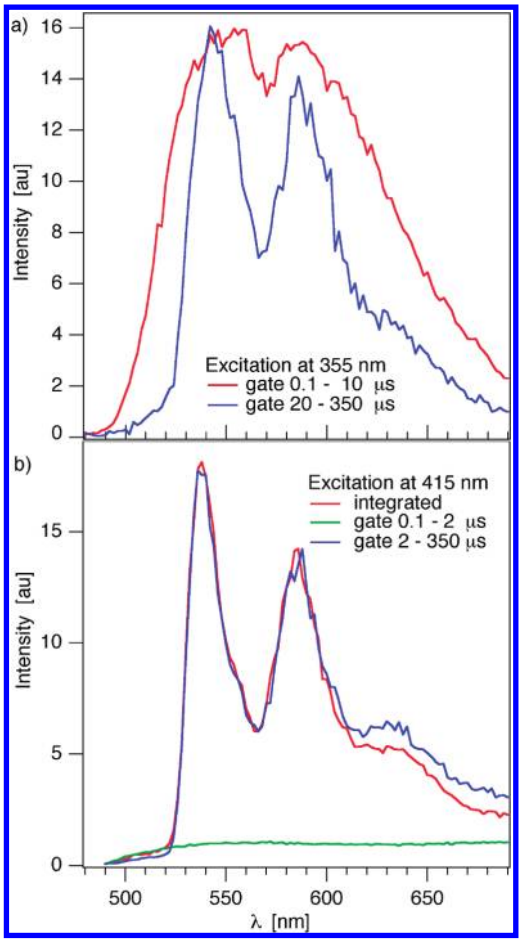

Figure 5. Time-gated luminescence spectra of $\{[Au(CN)_2]_2\mathbf{DNP}\}\cdot 4H_2O$ at 10 K, (a) excitation at 355 nm, gates 0.1−10 μs and 20−350 μs, (b) excitation at 415 nm, gates 0.1−2 μs and 2−350 μs, for comparison the integrated luminescence spectrum is included. All spectra not corrected for spectral response.

containing gold centers.[17f,g] As mentioned above, the structured bands in absorption and emission must involve the $\mathbf{DNP}^{2+}$ cations. The emission spectrum shows a progression in the aromatic ring frequency, and together with the long lifetime and the gap between excitation, the structured emission can be attributed to a $^3\pi\pi^*$ transition localized on $\mathbf{DNP}^{2+}$, which get its intensity via efficient intersystem crossing as a result of the heavy atom effect caused by the neighboring gold centers. The corresponding excitation spectrum with its four peaks is not straightforward to interpret, as it does not show a clear progression. In fact it looks like two transitions each with one quantum of a vibrational sideband. This could be because the two dinitro-benzene groups are not crystallographically equivalent. However, the bands only appear in the more sensitive excitation spectrum and must therefore correspond to forbidden transitions. We may thus tentatively assign these transitions to a $^3\pi\pi^*$ or $^1n\pi^*$ transition or transitions on $\mathbf{DNP}^{2+}$, possibly involving intramolecular charge transfer.

The luminescence centered at 580 nm attributed to the gold dimer upon excitation at 355 nm is only observable at the lowest temperature and quickly becomes quenched as the temperature is increased to above 50 K. In principle, this could be due to energy or electron transfer quenching. However, energy transfer to lower lying states involving $\mathbf{DNP}^{2+}$ can be ruled out on the grounds that the transition is missing in both emission as well as excitation spectra above 50 K (Figure 7 and Supporting Information, Figure S5).

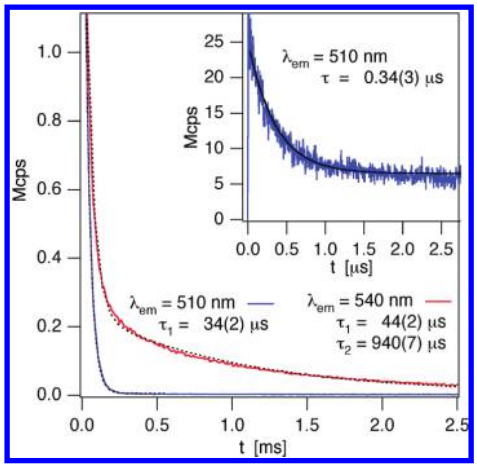

Figure 6. Luminescence decay curves of $\{[Au(CN)_2]_2\mathbf{DNP}\}\cdot 4H_2O$ at T = 10 K for excitation at 355 nm with detection at 510 nm (blue), and 540 nm (red). Inset: expanded view of the first 2.5 μs for detection at 510 nm,.

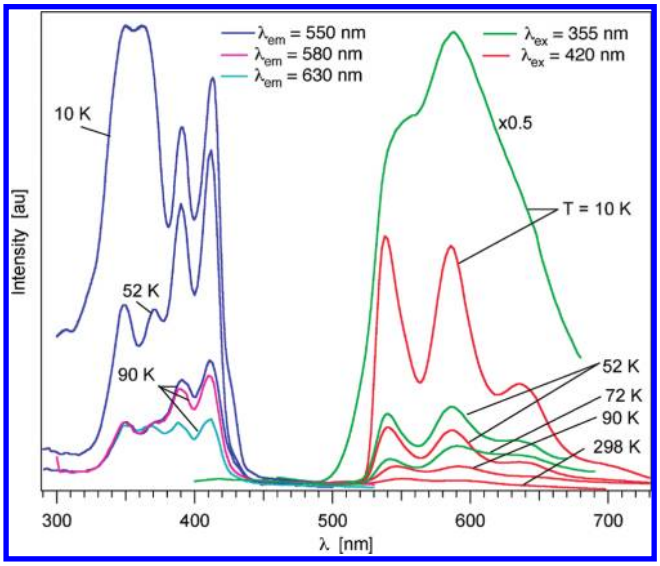

Figure 7. Excitation and luminescence spectra of $\{[Au(CN)_2]_2\mathbf{DNP}\}$ showing the disappearance of the broad excitation profile as well as the high- and low-energy emission profiles resulting from the $[Au(CN)_2]$ dimers at $T \geq 52$ K.

It is also not very likely given the spin-forbidden nature of the $\mathbf{DNP}^{2+}$ transition and energetically not feasible as the emission of the gold dimer is at too low an energy. Therefore, the quenching of the broad luminescence can be attributed to oxidative electron transfer in the excited state at higher temperatures. That is, at temperatures above 50 K, the small energy barrier can be overcome, so that an electron jumps from the initially excited state of the gold dimer to the viologen part, which acts as a trap, thus quenching the gold luminescence. The driving force for such an electron transfer is not very large and it seems that only a little thermal activation is needed for it to occur. The driving force for the back electron transfer on the other hand is large and immediately restores the overall ground state of the system without any additional luminescence. On the other hand, the viologen luminescence upon excitation at 410 nm is still observable at higher temperatures as the oxidizing power even of the excited viologen is not sufficient to oxidize $[Au(CN)_2]^-$ in its ground state. Figure 8 schematically

dx.doi.org/10.1021/ic201109u | Inorg. Chem. 2012, 51, 1294−1301

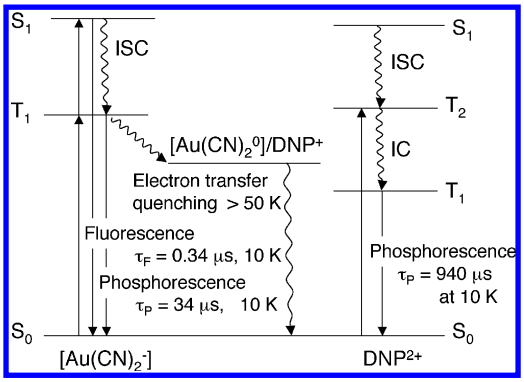

Figure 8. Energy diagram of the two emissive species. At higher temperature electron transfer quenches the $[Au(CN)_2]^-$ centered luminescence. S_0, ground state; S_1, first excited singlet state; T_1, T_2, first and second triplet states; IC, internal conversion; ISC, intersystem crossing.

summarizes the proposed energy level scheme and the dominant relaxation processes.

The role of the UV emission centered at 380 nm upon irradiation below 340 nm and tentatively attributed to the dicyanoaureate cluster is not very clear. It too becomes quenched quickly at higher temperatures, but in contrast to the 580 nm band, energy transfer quenching cannot be excluded. Also, one would expect a somewhat shorter lifetime for a higher excited dicyanoaureate state, given the large spin−orbit coupling and expected efficient intersystem crossing.

CONCLUSIONS

In the system under consideration, we have combined the linear inorganic $[Au(CN)_2]^-$ complex with a redox-active viologen derivative to form a supramolecular crystalline material with well-defined dicyanoaureate dimers. In these dimers, the linear complexes are close to parallel to each other, and the dimers themselves are well separated from each other by the large organic moieties. The structural information from X-ray crystallography can be correlated with the photophysical properties of the title compound $\{[Au(CN)_2]_2\mathbf{DNP}\}\cdot 4H_2O$. A fundamental issue that we are trying to address in our photophysical study of this compound is the unusual, low energy, *phosphorescence* displayed by both the $[Au(CN)_2]^-$ dimers and the **DNP** viologen moiety, given that the latter does not display any luminescence in its free state, and its methyl analogue is even used as luminescence quencher for many luminescent compounds[15] including gold-containing coordination complexes.[15i] We attribute this interesting observation to the heavy atom effect induced by the neighboring gold center displaying large spin−orbit coupling, with slight gold-viologen orbital overlap. This is expected for the **DNP** viologen with its extended π-conjugated phenyl peripheries in place of the two methyl groups of methyl viologen. We believe the interaction between the **DNP** moiety and the dicyanoaurate dimers to be sufficient to cause the originally nonfluorescing **DNP** to display unusual phosphorescence in the visible range induced by the neighboring heavy gold atoms. We expect further interesting results by combining **DNP** with other anionic transition metal complexes with perhaps better electron donating properties and lower oxidation potentials such as dicyanoargentate or ferrocyanide. However, the combination with the former, which would indeed allow a direct comparison with the dicyanoaurate, has not been successful to date.

ASSOCIATED CONTENT

Supporting Information

Powder X-ray Diffractogram, IR, electronic absorption and excitation spectra data of $\{[Au(CN)_2]_2\mathbf{DNP}\}\cdot 4H_2O$. This material is available free of charge via the Internet at http://pubs.acs.org.

AUTHOR INFORMATION

Corresponding Author

*E-mail: annie.powell@kit.edu (A.K.P.).

ACKNOWLEDGMENTS

This work was supported by the DFG (Center for Functional Nanostructures) and the Swiss National Science Foundation (Contract 200020-125175). The work of H.H.P., F.B.R., and X.L. were supported by the U.S. National Science Foundation (CHE-0315877). We thank C. Besnard for measuring the powder diffractogram.

REFERENCES

(1) (a) Leznoff, D. B.; Xue, B. Y.; Batchelor, R. J.; Einstein, F. W. B.; Patrick, B. O. *Inorg. Chem.* **2001**, *40*, 6026.

(2) (a) Kurmoo, M.; Day, P.; Mitani, T.; Kitagawa, H.; Shimoda, H.; Yoshida, D.; Guionneau, P.; Barrans, Y.; Chasseau, D.; Ducasse, L. *Bull. Chem. Soc. Jpn.* **1996**, *69*, 1233. (b) Chasseau, D.; Guionneau, P.; Rahal, M.; Bravic, G.; Gaultier, J.; Ducasse, L.; Kurmoo, M.; Day, P. *Synth. Met.* **1995**, *70*, 945. (c) Fujiwara, H.; Kobayashi, H. *Chem. Commun.* **1999**, *23*, 2417. (d) Kurmoo, M.; Pritchard, K. L.; Talham, D. R.; Day, P.; Stringer, A. M.; Howard, J. A. K. *Acta Crystallogr.* **1990**, *B46*, 348.

(3) (a) Mason, W. R. *J. Am. Chem. Soc.* **1973**, *95*, 3573. (b) Nagasundaram, N.; Roper, G.; Biscoe, J.; Chai, J. W.; Patterson, H. H.; Blom, N.; Ludi, A. *Inorg. Chem.* **1986**, *25*, 2947.

(4) (a) Chastain, S. K.; Mason, W. R. *Inorg. Chem.* **1982**, *21*, 3717. (b) Mason, W. R. *J. Am. Chem. Soc.* **1976**, *98*, 5182. (c) Carvajal, M. A.; Alvarez, S.; Novoa, J. J. *Theor. Chem. Acc.* **2006**, *116*, 472. (d) Katz, M. J.; Leznoff, D. B. *J. Am. Chem. Soc.* **2009**, *131*, 18435.

(5) (a) Hettiarachchi, S. R.; Schaefer, B. K.; Yson, R. L.; Staples, R. J.; Irmer, R. H.; Patterson, H. H. *Inorg. Chem.* **2007**, *46*, 6997. (b) Omary, M. A.; Colis, J. C. F.; Larochelle, C. L.; Patterson, H. H. *Inorg. Chem.* **2007**, *46*, 3798. (c) Omary, M. A. R.; Larochelle, C. L.; Patterson, H. H. *Inorg. Chem.* **2000**, *39*, 4527. (d) Colis, J. C. F.; Staples, R.; Tripp, C.; Labrecque, D.; Patterson, H. H. *J. Phys. Chem. B* **2005**, *109*, 102.

(6) (a) Lefebvre, J.; Tyagi, P.; Trudel, S.; Pacradouni, V.; Kaiser, C.; Sonier, J. E.; Leznoff, D. B. *Inorg. Chem.* **2009**, *48*, 55. (b) Agusti, G.; Gaspar, A. B.; Muñoz, M. C.; Real, J. A. *Inorg. Chem.* **2007**, *46*, 9646.

(7) Cramer, R. E.; Smith, D. W.; VanDoorne, W. *Inorg. Chem.* **1998**, *37*, 5895.

(8) (a) Katz, M. J.; Ramnial, T.; Yu, H. Z.; Leznoff, D. B. *J. Am. Chem. Soc.* **2008**, *130*, 10662. (b) Omary, M A. R.; Omary, M. A.; Patterson, H. H.; Fackler, J. P. Jr. *J. Am. Chem. Soc.* **2001**, *123*, 11237. (c) Lu, H.; Yson, R.; Ford, J.; Tracy, H. J.; Carrier, A. B.; Keller, A.; Mullin, J. L.; Poissan, M. J.; Sawan, S.; Patterson, H. H. *Chem. Phys. Lett.* **2007**, *443*, 55. (d) Guo, Z.; Yson, R. L.; Patterson, H. H. *Chem. Phys. Lett.* **2007**, *445*, 340.

(9) (a) Nagamura, T.; Muta, S.; Shiratori, K. *Chem. Phys. Lett.* **1995**, *238*, 353. (b) Nagamura, T.; Sakai, K. *J. Chem. Soc., Faraday Trans. I* **1988**, *84*, 3529. (c) Nagamura, T. *Pure. Appl. Chem.* **1996**, *68*, 1449. (d) Kuwabara, T.; Sugiyama, M.; Nanasawa, M. *Photochem. Photobiol.* **2001**, *73*, 469. (e) Lee, C.; Moon, M. S.; Park, J. W. *J. Inclusion Phenom. Mol. Recognit. Chem.* **1996**, *26*, 219.

(10) (a) Abouelwafa, A. S.; Mereacre, V.; Balaban, T. S.; Anson, C. E.; Powell., A. K. *CrystEngComm* **2010**, *12*, 94. (b) Yi, X. Y.; Wu, L. Z.; Tung, C. H. *J. Phys. Chem. B* **2000**, *104*, 9468. (c) Alam, M. M.; Ito, O. *J. Phys. Chem. A* **1999**, *103*, 1306. (d) Sullivan, B. P.; Dressick, W. J.; Meyer, T. J. *J. Phys. Chem.* **1982**, *86*, 1473. (e) Park, Y. S.; Lee, E. J.;

Chun, Y. S.; Yoon, Y. D.; Yoon, K. B. *J. Am. Chem. Soc.* **2002**, *124*, 7123. (f) Jiang, D. L.; Choi, C. K.; Honda, K.; Li, W. S.; Yuzawa, T.; Aida, T. *J. Am. Chem. Soc.* **2004**, *126*, 12084. (g) Ozawa, H.; Haga, M. A.; Sakai, K. *J. Am. Chem. Soc.* **2006**, *128*, 4926. (h) Ebbesen, T. W.; Ferraudi, O. *J. Phys. Chem.* **1983**, *87*, 3717.

(11) (a) Cummins, D. *J. Phys. Chem. B.* **2000**, *104*, 11449. (b) Grätzel, M. *Nature* **2001**, *409*, 575. (c) Lanzo, J.; De Benedittis, M.; De Simone, B. C.; Imbardelli, D.; Formoso, P.; Manfredi, S.; Chidichimo, G. *J. Mater. Chem.* **2007**, *17*, 1412.

(12) (a) Peon, J.; Tan, X.; Hoerner, J. D.; Xia, C.; Luk, Y. F.; Kohler, B. *J. Phys. Chem. A* **2001**, *105*, 5768. (b) Alvaro, M.; Facey, G. A.; Garcia, H.; Garcia, S.; Scaiano, J. C. *J. Phys. Chem.* **1996**, *100*, 18173. (c) Alvaro, M.; Garcia, H.; Garcia, S.; Marquez, F.; Scaiano, J. C. *J. Phys. Chem. B* **1997**, *101*, 3043. (d) Villemure, G.; Detellier, C.; Szabo, A. G. *J. Am. Chem. Soc.* **1986**, *108*, 4658.

(13) (a) Xu, G.; Guo, G.; Wang, M.; Zhang, Z.; Chen, W.; Huang, J. *Angew. Chem., Int. Ed.* **2007**, *46*, 3249. (b) Suzuki, M.; Kimura, M.; Hanabusa, K.; Shirai, H. *Chem. Commun.* **1997**, 2061. (c) Nagamura, T.; Sakaguchi, H.; Muta, S.; Ito, T. *Appl. Phys. Lett.* **1993**, *63*, 2762. (d) Yasuda, A.; Seto, J. *J. Appl. Electrochem.* **1988**, *333*, 5. (e) Samar, K. D.; Prabir, K. D. *Langmuir* **1998**, *14*, 5121. (f) Yoon, K. B.; Kochi, J. K. *J. Phys. Chem.* **1991**, *95*, 3780. (g) Hubig, S. M.; Kochi, J. K. *J. Phys. Chem.* **1995**, *99*, 17578. (h) Zhang, Q.; Wu, T.; Bu, X. H.; Tran, T.; Feng, P. Y. *Chem. Mater.* **2008**, *20*, 4170. (i) Königstein, C.; Spallart, M.; Bauer, R. *Electrochim. Acta* **1998**, *43*, 2435. (j) Andrade de Oliveira, L. A.; Haim, A. *J. Am. Chem. Soc.* **1982**, *104*, 3363.

(14) (a) Nagamura, T.; Sakai, K. *Chem. Phys. Lett.* **1987**, *141*, 553. (b) Nanasawa, M.; Miwa, M.; Hirai, M.; Kuwabara, T. *J. Org. Chem.* **2000**, *65*, 593. (c) Porter, W. W.; Vaid, T. P. *J. Org. Chem.* **2005**, *70*, 5028. (d) Casado, J.; Patchkovskii, S.; Zgierski, M. Z.; Hermosilla, L.; Sieiro, C.; Oliva, M. M.; López Navarrete, J. T. *Angew. Chem., Int. Ed.* **2008**, *47*, 1443. (e) Porter, W.; Vaid, T. P.; Rheingold, A. L. *J. Am. Chem. Soc.* **2005**, *127*, 16559. (f) Kelley, C. J.; Ansu, K.; Budisusetyo, W.; Ghiorghis, A.; Qin, Y.; Kauffman, J. M. *J. Heterocycl. Chem.* **2001**, *38*, 11.

(15) (a) El-Khouly, M. E.; Araki, Y.; Fujitsuka, M.; Ito, O. *Phys. Chem. Chem. Phys.* **2002**, *4*, 3322. (b) Ryu, S. Y.; Yoon, M.; Jeoung, S. C.; Song, N. *Photochem.Photobiol.Sci.* **2005**, *4*, 54. (c) Atik, S. S.; Thomas, J. K. *J. Am. Chem. Soc.* **1981**, *103*, 4367. (d) Prasad, D. R.; Ferraudi, G. *Inorg. Chem.* **1983**, *22*, 1672. (e) Lever, A. B. P.; Licoccia, S.; Ramaswamy, B. S.; Kandil, S. A.; Stynes, D. V. *Inorg. Chim. Acta* **1981**, *51*, 169. (f) Oddy, F. E.; Brovelli, S.; Stone, M. T.; Klotz, E. J. F.; Cacialli, F.; Anderson, H. L. *J. Mater. Chem.* **2009**, *19*, 2846. (g) Petersson, J.; Eklund, M.; Davidsson, J.; Hammarström, L. *J. Am. Chem. Soc.* **2009**, *131*, 7940. (h) Petersson, J.; Eklund, M.; Davidsson, J.; Hammarström, L. *J. Phys. Chem. B.* **2010**, *114*, 14331. (i) Shankar, K.; Marpu, S.; Yang, C.; Rawashdeh-Omary, M. A.; Omary, M. A. Abstracts of Papers, 239th ACS National Meeting, San Francisco, CA, United States, March 21−25, 2010, INOR−1087.

(16) Sheldrick, G. M. *Acta Crystallogr., Sect. A* **2008**, *64*, 112.

(17) (a) Schmidbaur, H. *Chem. Soc. Rev.* **1995**, 391. (b) Omary, M A. R.; Omary, M. A.; Patterson, H. H. *J. Am. Chem. Soc.* **2000**, *122*, 10371. (c) White-Morris, R. L.; Stender, M.; Tinti, D. S.; Balch, A. L.; Rios, R.; Attar, S. *Inorg. Chem.* **2003**, *42*, 3237. (d) Stender, M.; Olmstead, M. M.; Balch, A. L.; Rios, D.; Attar, S. *Dalton Trans.* **2003**, 4282. (e) Paraschiv, C.; Ferlay, S.; Hosseini, M. W.; Bulacha, V.; Planeixa, J. M. *Chem. Commun.* **2004**, 2270. (f) Ferrer, M.; Rodríguez, L.; Rossell, O.; Pina, F.; Lima, J. C.; Bardia, M. F.; Solans, X. *J. Organomet. Chem.* **2003**, *678*, 82. (g) Yoshida, Y.; Fujii, J.; Saito, G.; Hiramatsu, T.; Sato, N. *J. Mater. Chem.* **2006**, *16*, 724.